

Environmental performance of a metal-supported protonic ceramic cell and an electrolyte-supported solid oxide cell for steam electrolysis

*Original*

Environmental performance of a metal-supported protonic ceramic cell and an electrolyte-supported solid oxide cell for steam electrolysis / Moranti, A., Riva, F., Bachmann, T.M., Dailly, J.. - In: INTERNATIONAL JOURNAL OF HYDROGEN ENERGY. - ISSN 0360-3199. - 92:(2024), pp. 1284-1297. [10.1016/j.ijhydene.2024.10.221]

*Availability:*

This version is available at: 11583/2994719 since: 2024-11-23T15:20:31Z

*Publisher:*

PERGAMON-ELSEVIER SCIENCE LTD

*Published*

DOI:10.1016/j.ijhydene.2024.10.221

*Terms of use:*

This article is made available under terms and conditions as specified in the corresponding bibliographic description in the repository

*Publisher copyright*

(Article begins on next page)



# Environmental performance of a metal-supported protonic ceramic cell and an electrolyte-supported solid oxide cell for steam electrolysis

Andrea Moranti<sup>a,b</sup>, Federico Riva<sup>b</sup>, Till M. Bachmann<sup>b</sup>, Julian Dailly<sup>b,\*</sup>

<sup>a</sup> Politecnico di Torino, Corso Duca degli Abruzzi 24, 10129 Torino, Italy

<sup>b</sup> European Institute for Energy Research, Emmy-Noether-Str. 11, 76131 Karlsruhe, Germany

## ARTICLE INFO

Handling Editor: Dr V Palma

### Keywords:

Life cycle assessment  
Protonic ceramic cells (PCC)  
Hydrogen production/use  
Energy storage  
Steam methane reforming (SMR)

## ABSTRACT

Currently, higher shares of renewable electricity are promoted to reduce global Greenhouse Gas (GHG) emissions and decarbonize the energy sector. Electrolysis can help their integration into the grid but also for energy vector production.

In this context, Protonic Ceramic Electrolysis Cells (PCEC) are considered a promising clean energy technology. The ARCADE project focused on developing a cost-effective metal supported Protonic Ceramic Cell (PCC) reactor. Its environmental performance is compared to an existing Solid Oxide Electrolysis Cell (SOEC) using Life Cycle Assessment (LCA).

Results show that the faradaic efficiency heavily influences a PCC's environmental performance while manufacturing has minimal impact except for potential human health concerns from metal use. To get more detailed results, further studies on PCC performance, degradation and effect of scaling up from single cells to larger systems are needed but, already at the current state, PCCs show potential for clean energy.

## 1. Introduction

As the world's economy grows and energy consumption rises, renewable energy sources are seen as a potential solution to nevertheless decrease Greenhouse Gas (GHG) emissions. However, the intermittent nature and unpredictability of these sources pose challenges for grid stability. To address these issues, new technologies are needed to balance electricity production with storage and consumption, as well as producing chemical compounds for the hard to abate sectors [1]. Examining the available options, the electrochemical route and notably high temperature electrolysis (HTE) seems to be one of the most promising.

Solid Oxide Electrolysis Cells (SOEC) are one of the technologies belonging to this class. Steam is fed at the cathode side where it is split up into H<sub>2</sub> and oxygen ions O<sup>2-</sup> which migrate through the electrolyte to the anode where they are oxidized to molecular oxygen (O<sub>2</sub>) [2]. These cells typically operate at temperatures between 600 and 850 °C [3] and they are currently already commercially available with a Technological Readiness Level (TRL) of 7–8.

Besides SOEC, Protonic Ceramic Cells (PCC) gain significant attraction due to their cost-effectiveness and proton conductivity at moderate

temperatures, between 400 and 600 °C [4]. For these, the charge carriers are protons (H<sup>+</sup>): the inflow of steam and air is at the anode side with H<sub>2</sub>O being split into molecular oxygen, electrons and protons which migrate through the electrolyte toward the fuel electrode where they react with electrons into molecular hydrogen [5].

Due to the low TRL (3–4), the research is primarily focused on material-specific, single-cell investigations, with scant references linked to stack and especially system performance assessment [6].

SOEC and PCEC differ in materials used, cell pH-environment and operating temperature among other parameters. PCEC need less electrical energy per unit of hydrogen, with demonstrated efficiencies 14% higher than proton exchange membrane systems at high current density due to heat recuperation [7]. Synergies with other chemical synthesis processes can also be achieved [8].

However, the operation at elevated temperatures for both SOEC and PCEC leads to faster material degradation than for PEM, decreasing the cell's efficiency and thereby its hydrogen output per unit of electricity input.

From a high-level perspective, PCEC and SOEC present different advantages and disadvantages. First of all, the reactions require a lower activation energy due to the transmission of protons instead of oxygen

\* Corresponding author.

E-mail address: [Julian.Dailly@eifer.org](mailto:Julian.Dailly@eifer.org) (J. Dailly).

<https://doi.org/10.1016/j.ijhydene.2024.10.221>

Received 25 June 2024; Received in revised form 14 September 2024; Accepted 15 October 2024

Available online 31 October 2024

0360-3199/© 2024 The Authors. Published by Elsevier Ltd on behalf of Hydrogen Energy Publications LLC. This is an open access article under the CC BY license (<http://creativecommons.org/licenses/by/4.0/>).

ions, allowing faster reaction rates and requiring lower operating voltages. Hydrogen and water are kept separate in the two electrodes, not demanding further water removal from the produced hydrogen in electrolysis mode and decreasing the requirements, complexity and related cost of the post-treatment unit and ideally allowing to obtain directly high purity hydrogen. A higher theoretical efficiency due to the lower operating temperature can be reached. The lower temperatures required for the fluids at the inlet and outlet of each component also decrease the requisites for the Balance of Plant (BoP). A higher resistance to H<sub>2</sub>S poisoning is observed decreasing the requirements for desulphurization of the fuel especially if alternatives to pure hydrogen are fed to the cell when in fuel cell mode. The operating conditions also allow to reduce the degradation, and related stack replacement, maintaining high efficiencies. However, challenges remain in the anodic and cathodic reaction processes, sintering, conductivity, stability, durability and scale up of the cells [9].

The increase of TRL and scale up of the PCC, essential to achieve costs at the parity if not lower than for SOEC, may be assisted via cheaper reference materials and standardization of manufacturing processes [10].

Information on PCC is limited. Le et al. [11] provide information regarding scale up and stack integration for PCC technology. Available data for life cycle assessment is limited to specific elements (i.e. not on a system level) [12]. In this work, data is used for the PCEC coming from the ARCADE project and for SOEC from commercially available products [13]. Additionally, assumptions regarding BoP for the electrolysis mode are adopted from Robert et al. [14].

The cells studied in this work, in addition to the differences linked to PCEC and SOEC operation already discussed, also differ from each other due to the differences associated to their architecture, being the PCEC a metal supported cell and the SOEC an electrolyte supported. This aspect will also be linked, for each cell, with advantages and disadvantages in operation, manufacturing and development.

The metal supported cells, considered for the PCEC, are characterized by a porous metal substrate (typically made from ferritic stainless steel or other alloys) that serves as the structural support. The exploitation of this technology provides several advantages and disadvantages. Firstly, the metal structure offers mechanical stability and robustness reducing mechanical stresses as well as increasing the tolerance to thermal cycling thanks to higher thermal conductivity with respect to the ceramic materials. This makes it suitable also for fast start-up, shutdown and for more flexible operations [15–17]. Stability has been found to be improved also during redox cycling reaching higher lifetimes and reliability [15,17].

A metal layer as supporting material will also reduce the reliance on more expensive ceramic materials, reducing overall the expected cost also during future scale up of the technology. More in detail, this is related to reduced thicknesses of the layers especially in the membrane-electrode assembly (MEA). Specifically, the reduction of the electrolyte layer, which can also be deposited with alternative techniques, will guarantee lower losses and higher efficiencies during operation [16,17]. Also disadvantages related to the metal substrate can be found. Specifically increased corrosion and oxidation, when in wet and oxidizing

atmospheres. Issues can be found also in terms of compatibility with other materials, due to chromium volatilization that contaminate other layers worsening the performances [17]. This issue can be solved by the exploitation of protective layers which would increase the cost and production efforts.

Finally, metal supported architecture are obtained through complex manufacturing processes, due to additional interaction during co-sintering of metal and electrodes or electrolytes, with densification or melting of the metal substrate [16,17].

The electrolyte supported cell are being considered for the SOEC. In this architecture, the electrolyte layer provides the primary structural support. This technology has been exploited to operate at higher temperatures compared to the previous alternative, above 700 °C, in order to reach higher conductivities and efficiencies [17,18]. Despite the higher temperatures, the higher thickness of the electrolyte and its impact on the cell resistance and losses have to be accounted for. These operating conditions make the SOEC suitable for integration with available heat sources, such as those from industrial processes, making it suitable for hybrid systems and for specific high temperature applications [19]. However, the thicker layers and the use of a higher amount of ceramic materials causes higher costs for this technology. Still, this second technology benefits from a higher TRL and simpler manufacturing, making it a more viable option, at least at the current state, without requiring significant further development [18]. Additional information notably on the PCEC regarding cell, single repeating unit (SRU) and stack layers composition are provided by the ARCADE consortium combined to the performances.

The life cycle assessment of a technology or product provides a full determination of its environmental impacts, fundamental to avoid displacing environmental or health concerns to other locations or times, and also to avoid burden shifting among different environmental impacts [20]. Additionally, technologies that emit less GHG than their counterparts may still lead to higher impacts in other impact categories [21].

Several LCA studies, especially for high temperature solid oxide cell (SOC), have been published highlighting the impact that materials' production and supply, required for the manufacturing process, as well as emphasizing the importance of recycling at the end-of-life [22–25]. Still, the electricity and hydrogen consumption during the operation, respectively in electrolysis and fuel cell mode, were the most critical life cycle stage of all the life cycle.

In this study, a detailed assessment of one PCEC and one SOEC from manufacturing up to operation is performed. Different impact categories are evaluated to show the implications of using different materials in the membrane-electrode assembly or SRU. Also, when target performances are reached, the most critical life cycle stages are identified for different impact categories via contribution analysis. These are: manufacturing of the stack including all processes from the powder synthesis up to the assembly of the SRUs into a stack, the manufacturing of the BoP of the plant and the overall operation of the plant along its lifetime.

**Table 1**

Values used in the sensitivity analysis.

	SOEC - Main	PCEC - RES - 90-0.8	PCEC - RES - 60-0.8	PCEC - RES - 90-0.6	PCEC - RES - 60-0.6	PCEC - FR - 90-0.8	PCEC - DE - 90-0.8
Faradaic efficiency (%)	85%	90%	60%	90%	60%	90%	90%
Current density (A/cm <sup>2</sup> )	0.41	0.8	0.8	0.6	0.6	0.8	0.8
Stack power (kW)	2.33	2.27	3.45	2.27	3.41	2.27	2.27
SRU (#)	30	27	41	36	54	27	27
Electricity mix	PV (3 kW, roof mounted)	PV (3 kW, roof mounted)	PV (3 kW, roof mounted)	PV (3 kW, roof mounted)	PV (3 kW, roof mounted)	French	German

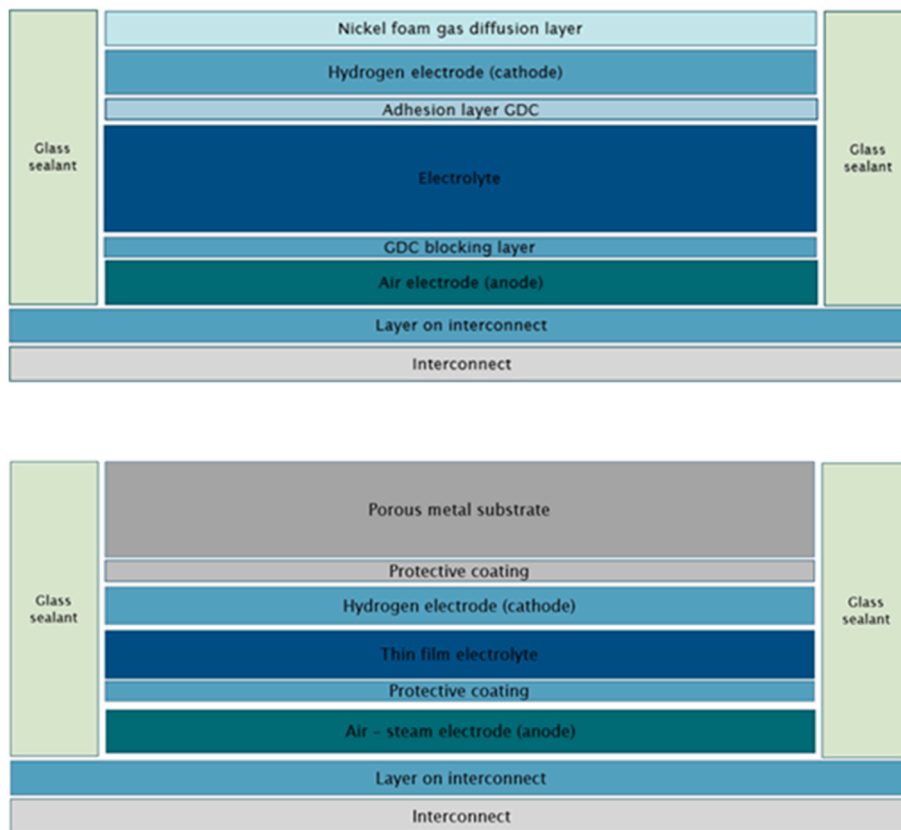


Fig. 1. SRU for SOEC technology (top) and PCEC technology (bottom).

2. Materials and methods

2.1. Life cycle assessment

A chain-based conventional (attributorial) LCA is carried out according to ISO 14040:2006 and ISO 14044:2006 standards and following the guidance documents by the EU’s Fuel Cell and Hydrogen Joint Undertaking [26]. The model is implemented with the Umberto LCA + software [27].

The goal of this LCA is to provide a comprehensive comparative environmental analysis between one commercially available SOEC and

one innovative, newly developed, metal supported PCEC. For a fair comparison between the more advanced and the newly developed cells, environmental hotspots are identified for the case that the PCEC target performances of 90% faradaic efficiency and a 0.8 A/cm<sup>2</sup> current density are achieved. These targets had been set by the ARCADE consortium composed of CNRS (ICGM-AIME, IMN and FEMTO-ST), EIFER, DLR, Ceraco and Air Liquide.

Primary data is used from the ARCADE project for the PCEC to the extent that it is available. Otherwise, data from the literature or from the commercial LCA database ecoinvent version 3.8.1 was used.

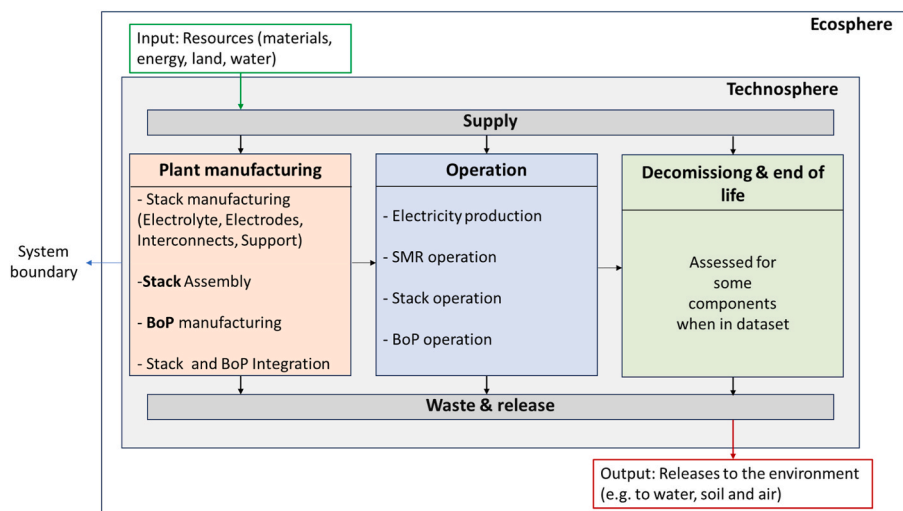


Fig. 2. Life cycle and system boundaries overview.

## 2.2. Systems analyzed

The newly developed PCEC is compared to a SOEC from Sunfire [13]. Their technical characteristics are described in Table 1.

SOEC and PCEC mainly differ in terms of the type of ions moving through the electrolyte [28,29]. For the SOEC, one set of data for its technical performance, stack structure and electricity source is evaluated, while for the PCEC a sensitivity analysis concerning electricity, faradaic efficiency and current density is carried out. Different combinations for these operating parameters are used which require modifying power and SRU number in order to produce the same amount of hydrogen over its lifetime from the hypothetical PCEC stack. The electricity source is also varied for the PCEC: it is either produced from a low-carbon renewable energy source (RES, i.e. photovoltaics, PV) or from a power generation mix with a low-carbon or higher-carbon intensity (France, FR, and Germany, DE).

In either case, cells are assembled into SRU, further joined into a stack and finally combined with the required balance of plant to make a complete system. The SRU structure of the SOEC is defined according to the Sunfire Hylink commercial stack [13] (bottom of Fig. 1). The structure of the PCEC SRU was defined by the ARCADE consortium (top of Fig. 1).

Both systems are assumed to operate in thermoneutral mode, for the same lifetime of forty thousands hours and using steam from Steam Methane Reforming (SMR) which is further heated up to 600 °C and 800 °C respectively for PCEC and SOEC by electric heaters. To what concerns power supply and hydrogen treatment systems, the “power supply system” is considered in both configurations [30,31]. The “hydrogen treatment system” is neglected because it is not necessary in the PCEC configuration, while the purification stage is considered for SOEC. It is modeled according to EIFER internal expertise or available literature [31–36].

## 2.3. System boundaries and cut-offs

A “cradle-to-gate” approach is taken. The LCA includes manufacturing, operation and maintenance of the two systems. Operation is considered continuous over the lifetime, neglecting maintenance due to lack of information. The utilization (including compression and storage) of the produced hydrogen is considered the same for the two systems and therefore outside the scope of this LCA. A summarizing scheme for the boundary and stages considered is shown in Fig. 2.

Decommissioning and the end-of-life stage are, due to lack of data, are assessed for some components covered by theecoinvent datasets used.

Due to the thermoneutral operation of the stack, the heat produced is used within the system and therefore not considered as a by-product. Furthermore, the produced oxygen is ventilated.

The SMR plant jointly produces electricity, hydrogen and steam. This multi-functionality is solved by energetic allocation according to the lower heating value (LHV).

The time-related reference are the years 2020 and 2023 or according to the most recent datasets available in ecoinvent v3.8.1. The geographic reference is Europe - or countries producing relevant supplies for Europe or global - with transport data often included in ecoinvent market type datasets. For further processed goods, additional transport data might be needed [37], not considered in this work.

Elementary flows, such as raw materials, water, solvents, transportation, electricity, energies, may be modeled considering the 5% cut off rule [26] and excluding those flows from the study which, though, is linked with some difficulties [38]. In order to apply this rule the cut-offs are calculated relative to the excluded environmental impact they would produce. To retrieve this value, an approximation of the total environmental impact has to be made or the whole system needs to be modeled to know how much 5% are. However, a complete model, with the associated efforts, will have to be established making the cut-off no

longer needed and therefore finally excluding from this work.

## 2.4. Life cycle impact assessment (LCIA)

The LCIA is performed according to ISO (14,044:2006) with the methodology Environmental Footprint (EF) 3.0 no long-term (LT) [39]. In year 2023 – at the time when modeling exercise was carried out - this was the most recent available in the UMBERTO software and most aligned with the European Commission’s Environmental Footprint methodology [35].

The investigated impact categories are selected depending on which components are analyzed.

- Main stack layers comparative analysis: climate change; abiotic depletion potential, material resources: metals/minerals; human toxicity: carcinogenic; water use: user deprivation potential; particulate matter formation;
- Stack layers comparison: acidification; climate change; ecotoxicity: freshwater; human toxicity: carcinogenic; ionizing radiation; human health; land use: soil quality index; material resources: metals/minerals; ozone depletion; particulate matter formation; water use: user deprivation potential.

## 2.5. Functional units and reference flows

The functional unit for the electrolyzer is defined as the production of 1 MJ of hydrogen, also simplifying comparison with other forms of energy [40]. The produced hydrogen has a Higher Heating Value and a Lower Heating Value respectively equals to 141.8 MJ/kg and 120 MJ/kg at 1 bar, 25 °C and 99.99% purity according to literature and technical reports [41,42]. The lower heating value has been used in this work.

Hydrogen production is kept constant over time along the full life cycle and is equal for PCEC and SOEC since the effect of degradation is accounted for during sensitivity analysis. The reference flow is the hydrogen produced over the lifetime of forty thousands hours, agreed in the ARCADE project’s consortium as target and also confirmed in literature [43], considering the productivity of the stack fixed in each case study, and evaluated through the values summarized in Table 1, as equal to 0.06 kg/h. The final value for the reference flow, evaluated by multiplying hourly flow rate for operating hours and lower heating values, amounts to a value of  $2.84 \cdot 10^5$  MJ.

## 2.6. Life cycle inventory and assumptions

The inventory relies on primary and secondary sources, such as databases and literature.

Main assumptions for the manufacturing processes are.

- Powder synthesis via the Pechini sol-gel method [44] through nitrates precursors. Due to lack of the chemical precursors datasets in the ecoinvent databases, they are modeled assuming chemical synthesis reaction. For example neutralization between acid and base, mostly using oxides, carbonates, nitric acid and water as done for example for commonly used calcium nitrates [45]. This approach has been selected also according to other studies available in literature and reports [46,47]. For Pechini sol-gel modeling, citric acid and ethylene glycol have been considered respectively as chelating and polymerizing agent with molar ratios of 1:4:1 for citric acid, ethylene glycol and nitrates [48]. The choice for these specific reactants, additives and ratios has been defined following a careful literature review [12,48–53].
- Layers manufacturing processes consisting of slip casting, useful to produce bodies with different geometries and sizes [25,54–57], screen printing, simple, flexible and economical technique [58–61] and physical vapor deposition allowing the application of thin films [62–65].

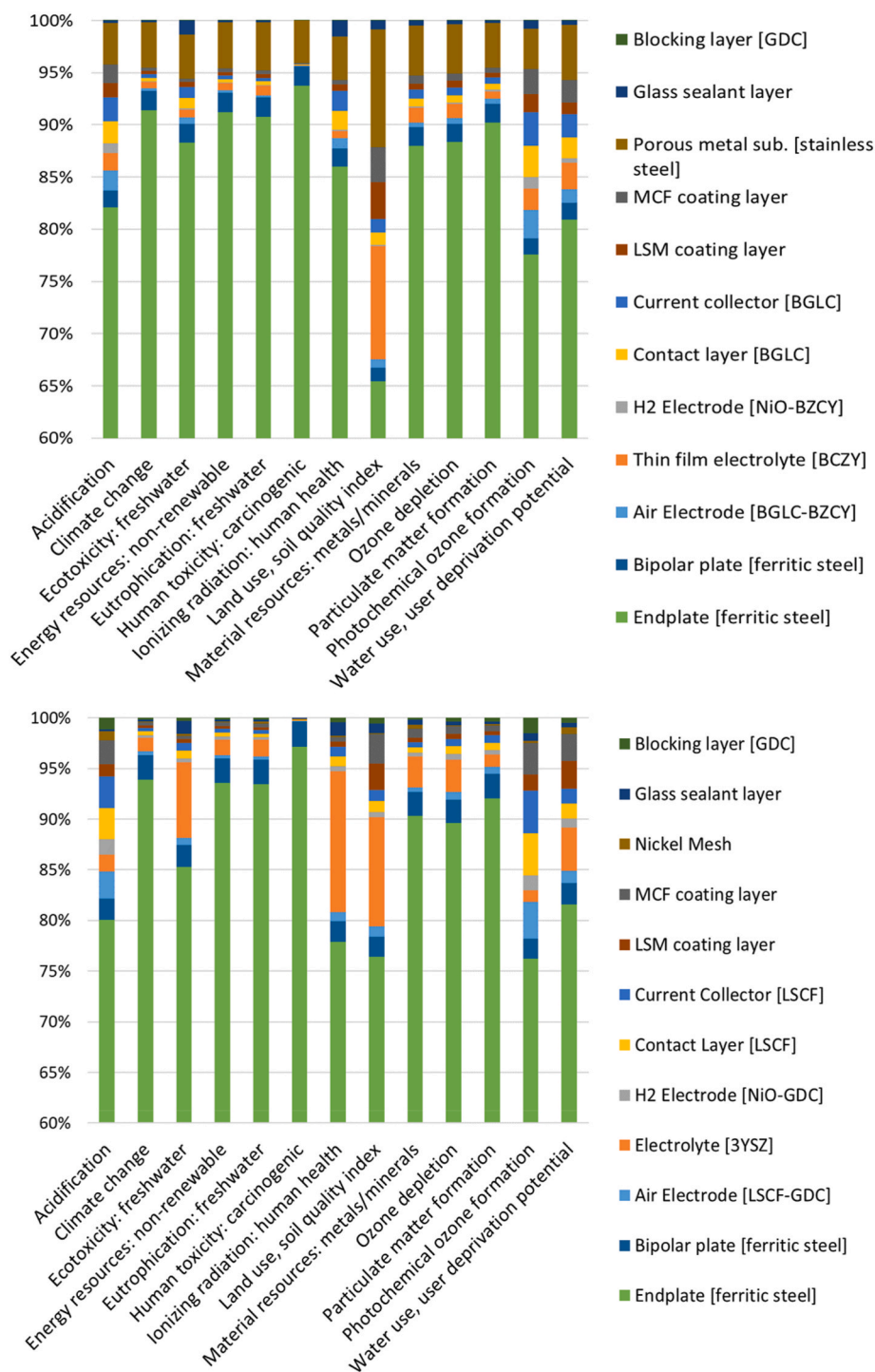


Fig. 3. Contribution analysis at stack level (all components): the PCEC (top) and SOEC (bottom) (only the contributions from the endplates above 60% shown).

- BoP (except for the hydrogen treatment system, see below): modeled according to a previous LCA study related to a proton exchange membrane electrolyzer developed at EIFER and therefore available according to internal expertise which also relies on other available studies and references [30,31,66,67]. The definition of the required components, consisting in here especially on the power supply system, and of additional assumptions derive also from other sources available in literature [67–70]. Information included in this study regarding the power supply system are hereafter described. A commercial transformer able to convert 480 VAC and with a maximum power of 500 kW weighs, when considering the cabinet, weight

1451 kg and is dependent on input power and maximum power [71, 72]. This weight has been rescaled to reach the characteristics of the reference stack [73] and is used as input for the model rescaling the ecoinvent dataset for the transformer (1 kg). In addition to the transformer also a rectifier is needed [30]. The ecoinvent dataset for an inverter (500 kW) is therefore used as a proxy by linearly rescaling it for the power required in this system. One hundred kilograms of both control electronics and copper for wiring and 300 kg of plastic (PVC) are further employed [31]. The environmental burden for these components in the ecoinvent database was rescaled to the evaluated nominal power. Finally electric heaters are also

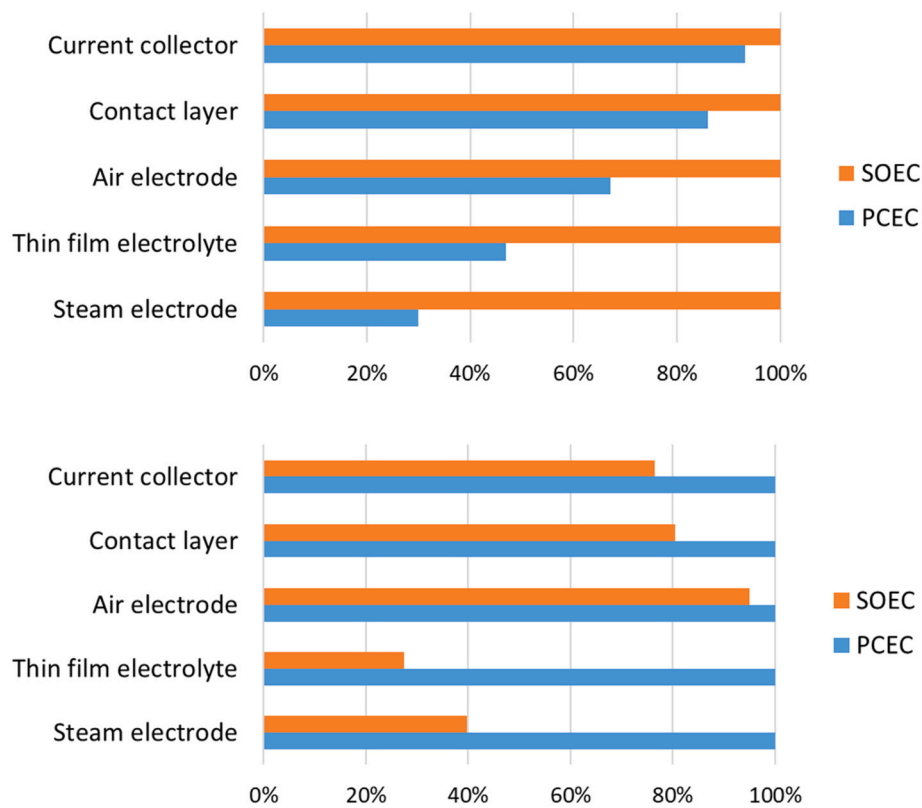


Fig. 4. Climate change, main stack layers comparative analysis normalized to the worst case on (top), additionally normalized to mass on (bottom).

linearly rescaled from theecoinvent dataset according to the required heating power for the streams. As defined all of the rescaling has been performed considering a unitary factor which can be considered as valid especially as rough estimation as made in several sectors in some cases only in terms of technical specifications [25,66]. This approach can also be justified by the low impact that the BoP has on the overall environmental performance of the system as also validated from other available studies in which plant construction is often neglected due to its small share on the overall assessment of the technology [67,74].

- hydrogen treatment system for the SOEC: the hydrogen treatment system of a PEM electrolyzer is used as a proxy also due to similarities except for the operating temperatures [31,74]. It consists of a water gas separator and de-oxo purifier. The water gas separator, for high efficiency filtration of non-corrosive flows [33], based on theoretical considerations experimentally confirmed and on products commercially available for other applications, it requires approximately 7 cm tank diameter for a 100 kg/day hydrogen production system [32,75]. According to this sources, as a rough estimation, the cross section is linearly rescaled to the daily hydrogen production of the system under study. A tank length of 2 m is assumed based on a real observation of the system installed at an EDF R&D facility and according to available literature. A standard thickness of 10 mm has also been used according to EIFER internal expertise and literature [76]. Tank and demister pad material for the separation are made of stainless steel [33,77]. The pad is assumed to have a thickness of 10 cm, from commercial available products [78], with a pad bulk density of 182 kg/m<sup>3</sup> [34]. After leaving the water gas separator, the hydrogen stream still contains approximately 800 ppm of oxygen [31] which is reduced in a de-oxo purifier through a platinum-group metal based catalytical recombination [35]. Hydrogen gas is passed over a bed of catalyst where oxygen reacts with hydrogen to form water that can be easily removed [31,79]. The sizing specification of available de-oxo manufacturers of

approximately 350 m<sup>3</sup>/h stream requires around 700 mm diameter and 920 mm height [36,80] again considering a thickness of 10 mm as for the water-gas separator and according to reference for hydrogen vessels [76].

The composition of the cell components and the associated manufacturing techniques are summarized for SOEC and PCEC in tables available in the supplementary information.

For all the plants, the inverter is assumed to be replaced every 10 years also considering lower expected durability since connected to a PV plant [81,82]. Furthermore, in order to model the photovoltaic energy production, the 3 kW peak, roof mounted photovoltaic systems ecoinvent dataset was used.

### 3. Results and discussion

The LCA results are presented first for the stack manufacturing and then for the full life cycle.

#### 3.1. Stack manufacturing

The endplates contribute about 80% and up to 95% for most impact categories for both technologies (and at least 65%) (Fig. 3). This is due to the substantial mass contribution compared to other layers (Tables in supplementary information).

For the PCEC, following the interconnectors, the porous metal substrate contributes the most (between 4% and 11.5%) due to its overall mass.

Besides the endplates, the bipolar plates and the electrolyte contribute second and third to all impact categories for SOEC. Being also structural elements, they are again the ones with the highest thickness and mass contribution.

More into detail, the stainless-steel bipolar plate strongly contributes to the "Human toxicity: carcinogenic" impact category (7.1%) due to

**Table 2**

Most contributing items contributing together at least 60% to the impact category results of a given technology's layer (1,2,3: contribution of first, second and third rank order).

Layer	Item (alphabetical)	Climate change		Acidification		Human toxicity: carcinogenic	
		SOEC	PCEC	SOEC	PCEC	SOEC	PCEC
<u>Current collector</u>	Citric acid	1	1	1	1		
	Cobalt oxide			3	3	1	1
	Gadolinium oxide		2		2		2
	Lanthanum oxide	2		2		2	
<u>Contact layer</u>	Citric acid	1	1	1	1		
	Cobalt oxide			3	3	1	1
	Gadolinium oxide		2		2		2
	Lanthanum oxide	2		2		2	
<u>Electrolyte</u>	Barium oxide						3
	Citric acid		2		1		2
	Electricity		1		2	2	1
	Urea	2		2			
	Yttrium oxide	1		1		1	
<u>Air electrode</u>	Citric acid	1	1	1	1		1
	Cerium oxide	3		3			
	Cobalt oxide					1	
	Gadolinium oxide		2		2		2
	Lanthanum oxide	2		2		2	
<u>Fuel electrode</u>	Butyl acetate	1		1	1		
	Cerium oxide						
	Citric acid	3	1	3		2	2
	Nickel oxide	2	2	2	2	1	1

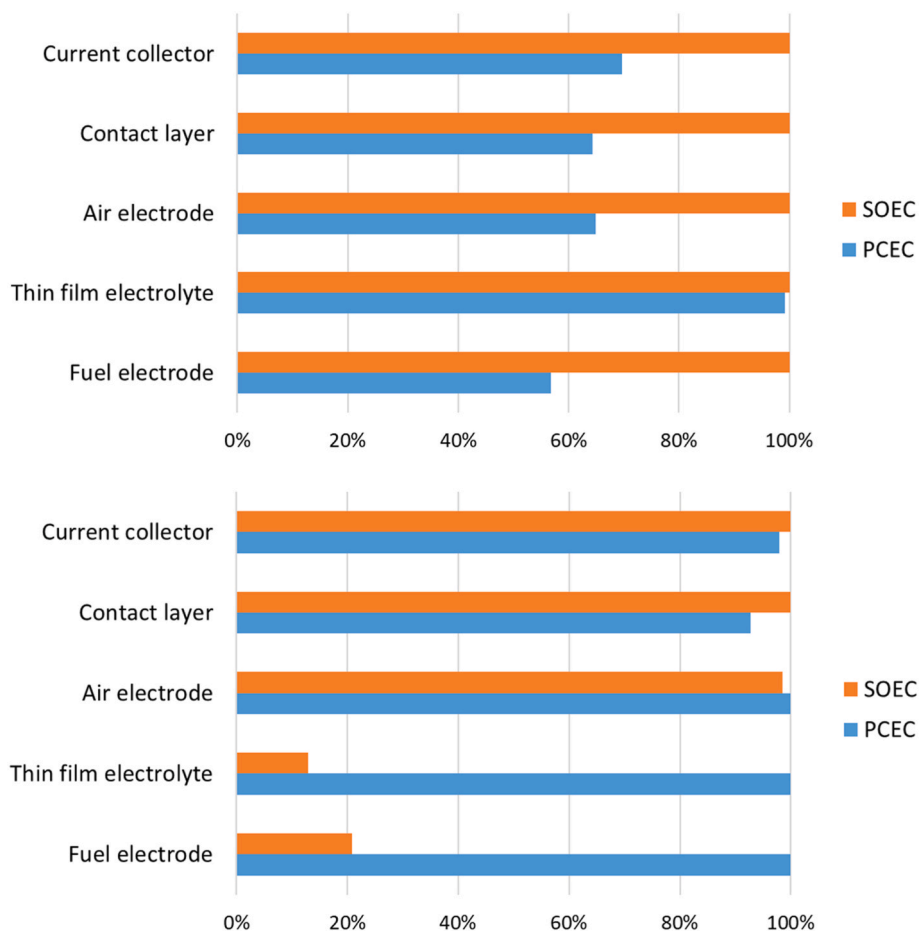


**Fig. 5.** Acidification, main stack layers comparative analysis normalized to the worst case (top), additionally normalized to mass (bottom).

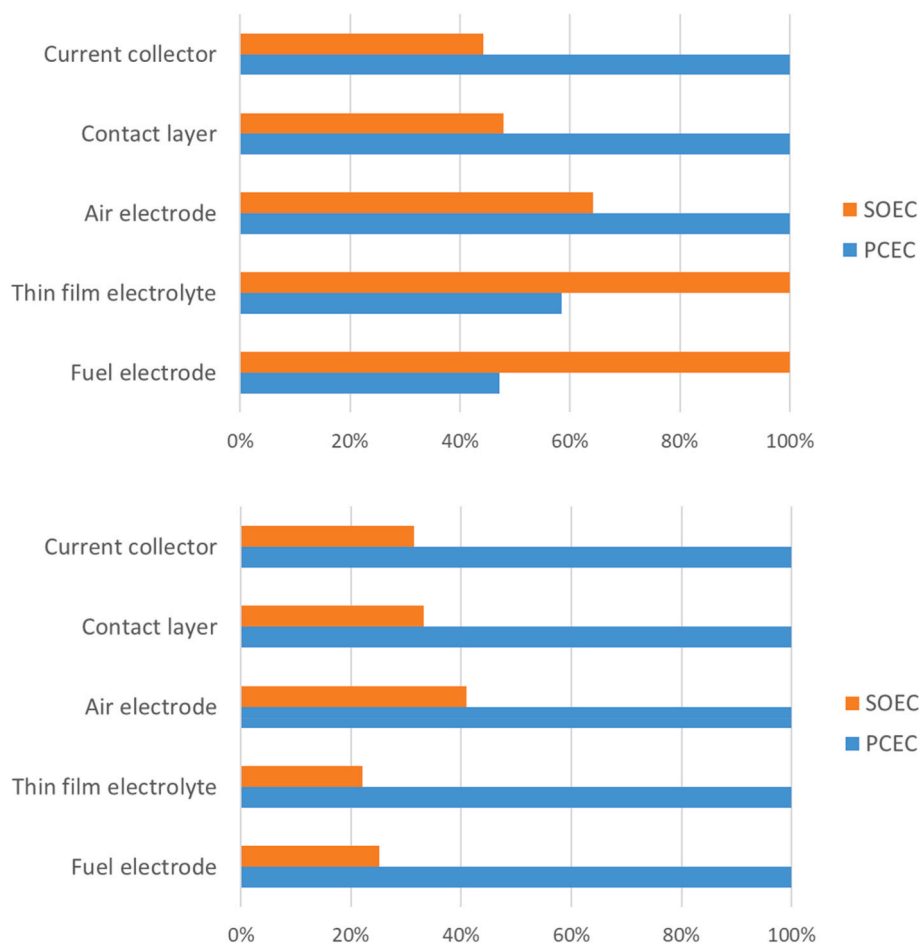


Fig. 6. Human toxicity, main stack layers comparative analysis normalized to the worst case on (top), additionally normalized to mass on (bottom).

presence of chromium, arsenic and nickel. Regarding other impact categories such as acidification and photochemical ozone formation, a different pattern can be highlighted despite the higher thickness of the electrolyte compared to the other elements. These differences are associated with the nitrogen oxide emissions, main contributor to the said categories of acidification and photochemical ozone formation, which are mainly linked to the nitrates production used for the synthesis of powders and not required instead in the electrolyte manufacturing process which employed directly oxides.

To better understand differences in the environmental profiles, a comparative analysis for the main layers differing among the two technologies is carried out. Results are presented for specific impact categories whose patterns are similar to other impact categories (indicated in brackets if applicable): Climate change (eutrophication of fresh water, particulate matter formation, ozone depletion potential), Acidification, Human toxicity: Carcinogenic (water use, land use, material resources; the main numeric results are available in tables in the supplementary information). It is important to note that, while the patterns might be the same, the materials and constituents that contribute most vary for different impact categories.

The results are internally normalized to the worst performing layer in absolute terms first and then additionally in specific terms (i.e. per layer mass).

### 3.1.1. Climate change (similar: eutrophication of fresh water - particulate matter formation - ozone depletion potential)

In absolute terms, SOEC layers show higher climate change impacts compared to the PCEC one (top of Fig. 4). The opposite is true when normalizing the results to the layers' mass (bottom of Fig. 4). The main

contributors, together contributing at least 60% to the impact category results of a given technology's layer, are (see Table 2): Citric acid and Lanthanum oxide (SOEC) or Citric acid and Gadolinium oxide (PCEC) for the current collector, contact layer and air electrode; for the electrolyte, Yttrium oxide and urea for SOEC, and Electricity and Citric acid for PCEC; and for the fuel electrode, Butyl acetate, Citric acid and Cerium oxide for SOEC, and Citric acid and Nickel oxide (NiO) for PCEC. This is because the SOEC layers are heavier than the PCEC layers despite involving materials for which the associated GHG emissions are smaller.

The electrolyte shows the most substantial change due to the different architecture used for the cell: in contrast to the PCEC, the SOEC is an electrolyte supported cell. Also related to architecture, the electrolyte of the SOEC's fuel electrode also includes the diffusion layer. Furthermore, a lower amount of citric acid in the Pechini process is required for the gadolinium-doped ceria (GDC), used in SOEC, when compared to the barium cerium yttrium zirconate (BZCY), employed in PCEC. Finally, the manufacturing processes differ between the two cells.

### 3.1.2. Acidification

In absolute terms, the SOEC layers lead to substantially higher acidification impacts than the PCEC layers, except for the thin film electrolyte (top of Fig. 5). In per mass terms (bottom of Fig. 5), the contact layer and current collector are the layers showing a higher impact for SOEC than for PCEC. Contrarily, the PCEC layers thin film electrolyte and fuel electrode are more impacting than those of the SOEC.

Again, as already previously stated and as further highlighted in Table 2, the powder synthesis process, characterized by the use of citric acid, is the most affecting parameter with a higher amount of citric acid

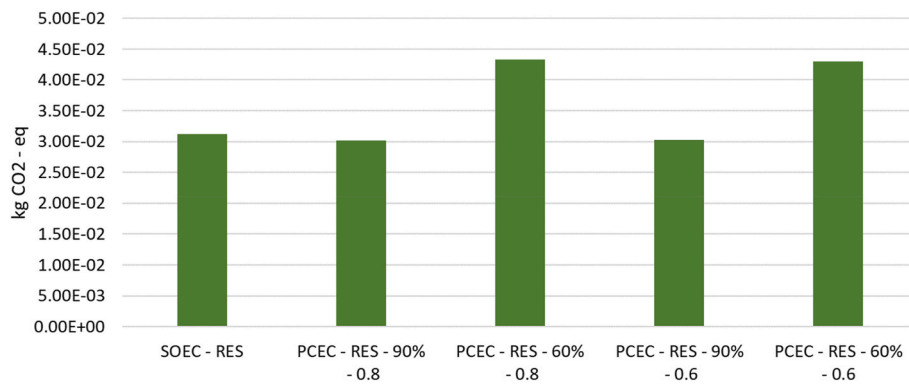


Fig. 7. Comparison of GHG emission results along the full life cycle for all the analyzed cases with PV as electricity source.

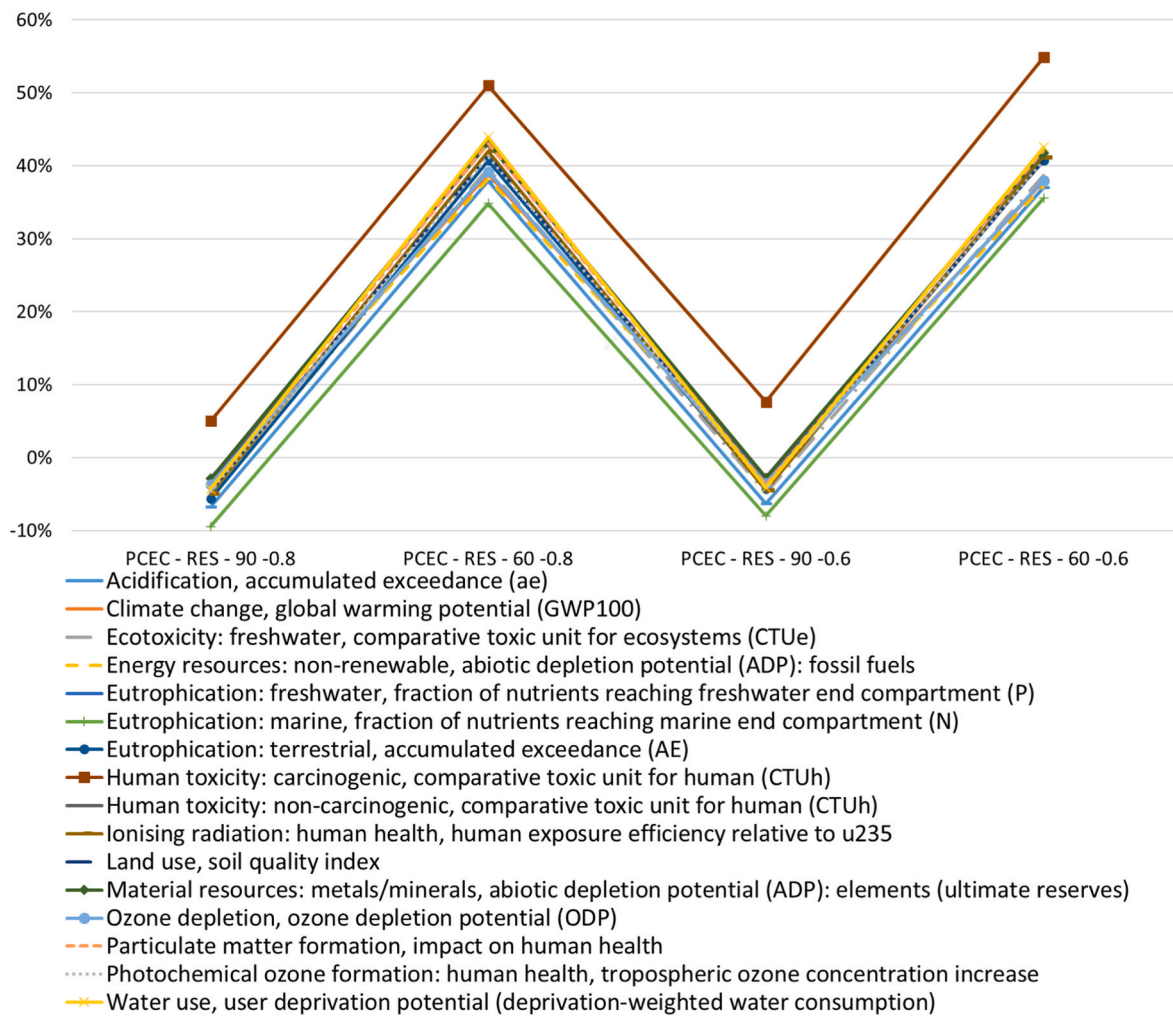


Fig. 8. Variation of LCIA results for the different analyzed PCEC cases relative to the SOEC base case when relying on electricity from PV ((PCEC-SOEC)/SOEC).

used in the lanthanum strontium cobalt ferrite (LSCF), used in SOEC, compared to the barium gadolinium lanthanum cobalt (BGLC), employed in PCEC. For the air electrode, this effect is softened by the use of the composite LSCF-GDC (SOEC) needing less citric acid than the BGLC-BZCY (PCEC) as previously explained.

3.1.3. Human toxicity (similar: water use - land use - material resources)

Regarding the “human toxicity” impact category, yet another pattern can be observed. Here, the SOEC’s electrolyte and fuel electrode lead to a higher impact when looking at the absolute values (top of Fig. 6).

However, when normalized to mass, all PCEC layers lead to higher impacts than their corresponding SOEC layers. The main contributors are summarized in Table 2.

3.2. Full life cycle

The environmental performance of SOEC and PCEC over their full life cycles has been evaluated, by also varying main performance related parameters of the PCEC, as summarized in Table 1.

While all impact categories have been analyzed (see detailed results

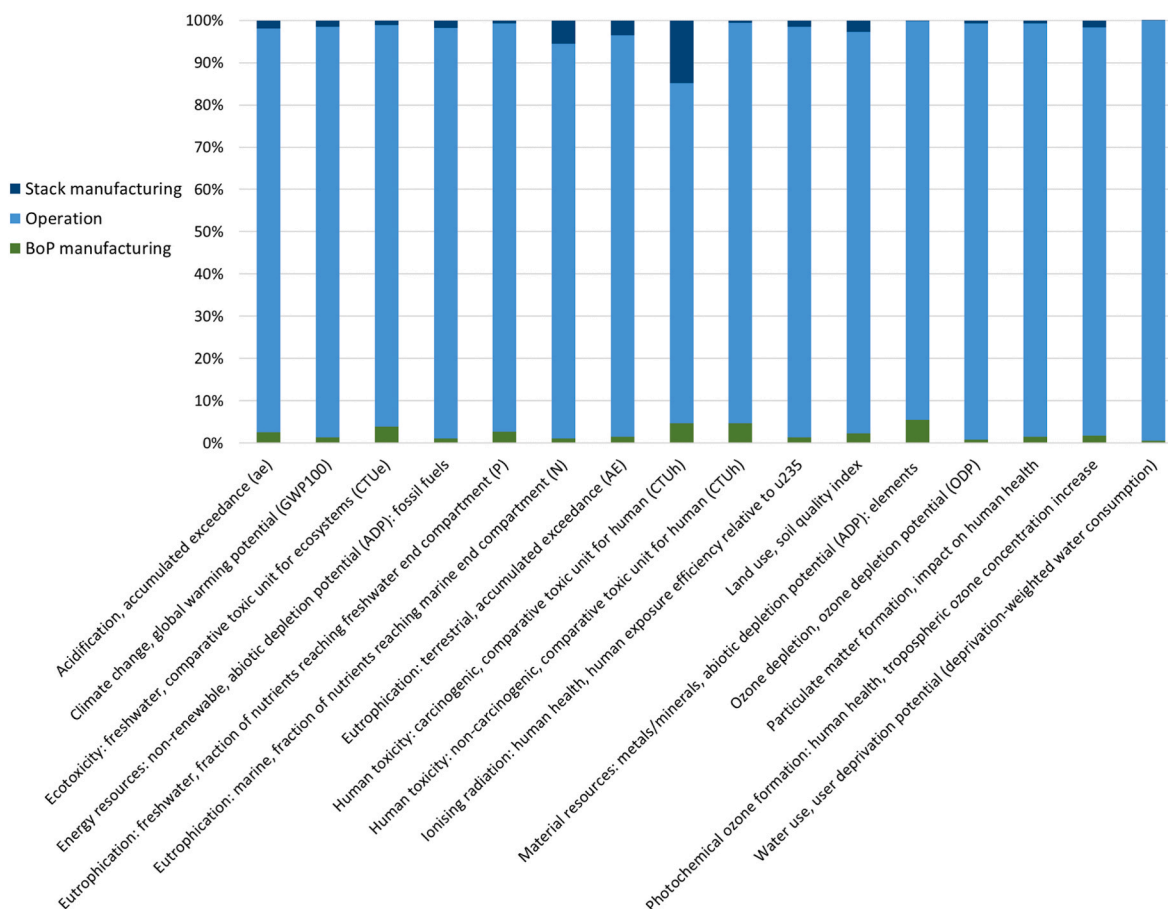


Fig. 9. Contribution analysis for the different life cycle stages in the case “PCEC – RES – 90–0.8” (i.e. performance targets are reached).

in the supporting information), results are first presented for the “Climate change” impact category (Fig. 7).

Renewable electricity input, assumed to be produced by a roof-PV, is considered in every of the analyzed cases. Water consumption is stoichiometrically determined from the hydrogen production target which is equal in both systems. Therefore, it results to be the same among SOEC and PCEC in every analyzed case.

Fig. 7 shows that when the faradaic efficiency reaches the 90% target value, environmental impacts are comparable to SOEC. A higher decrease of the current density principally affects the number of SRU needed to produce the same amount of hydrogen as well as impacting the electricity demand. The variation of this parameter mainly leads to a discrete increase in the number of SRU, which may account for a stack with a power demand higher than the minimum one which is ideally calculated from the required output hydrogen. While the number of SRU leads to a one-off increase in GHG emissions, the increased electricity demand concerns the whole operational life of the PCEC that in this case is provided by PV.

The percentile variation relative to SOEC is shown in Fig. 8 for each impact category and according to all renewable energy cases analyzed. The overall trend is similar in all scenarios. The PCEC impacts due to human toxicity are always the highest relative to SOEC due to the use of the metal support, original characteristic of the implemented PCEC technology. As highlighted in these figures, the faradaic efficiency has the strongest impact, in contrast to the operating current density.

The contribution of different life cycle stages (i.e. stack manufacturing, BoP manufacturing and electrolysis operation) to all impact categories is shown in Fig. 9. Results are shown for the reference PCEC case where performance target values (i.e. 90% faradaic efficiency and a 0.8 A/cm<sup>2</sup> current density) are assumed to be reached.

For almost all impact categories along the full life cycle, BoP and stack manufacturing show a negligible contribution relative to operation whose main contributors are the electricity consumed and the steam production. The only exception concerns “human-toxicity, carcinogenic” to which the stack manufacturing contributes approximately 15%. The contribution that the stack manufacturing has on the lifetime environmental impact, especially for the “human-toxicity, carcinogenic”, could vary if also the end-of-life was considered quantitatively (such as through different scenarios concerning reuse, recycling, energy extraction or landfill).

The main contributors to “human toxicity: carcinogenic” are mostly the same as for stack manufacturing.

To get a better understanding of the operation phase another sensitivity analysis was conducted, changing the electricity source from PV to the French or German electricity production mixes. For most of the main impact categories (i.e. material resources: metals/minerals, eutrophication of fresh water, human toxicity: carcinogenic with PV and German mix, water use: user deprivation potential), the electricity feed has the highest impact. Different outcomes are observed for climate change, acidification and human toxicity: carcinogenic if the French electricity mix is used, when the steam methane reforming phase becomes the one with higher environmental impact.

The effect of electricity sources other than PV on the main impact categories has been evaluated through a sensitivity analysis when target performances for the PCEC are reached. A variation relative to the PV case study is shown in Table 3.

The French electricity mix from 2021 is mainly composed of nuclear power. The use of this energy source, therefore, is responsible for.

- An increase in “ionizing radiation” up to +6000%

**Table 3**  
Effect of different electricity mixes on the environmental profile of the PCEC target case ((PCEC [FR/GE]-PCEC [RES])/PCEC [RES]).

LCIA IMPACT CATEGORY	Unit	PCEC - RES - 90-0.8	PCEC - FR - 90-0.8	PCEC - DE - 90-0.8
Acidification, accumulated exceedance (ae)	mol H <sup>+</sup> - eq	2.64E-04	-31.11%	66.49%
Climate change, global warming potential (GWP100)	kgCO <sub>2</sub> - eq	3.02E-02	-8.83%	429.98%
Ecotoxicity: Freshwater, comparative toxic unit for ecosystems (CTUe)	CTUe	1.81 E+00	-29.12%	13.07%
Energy resources: Non-renewable, abiotic depletion potential (ADP): Fossil fuels	MJ, net calorific value	4.50E-01	878.82%	497.73%
Eutrophication: Freshwater, fraction of nutrients reaching freshwater end compartment (P)	kg PO <sub>4</sub> - eq	4.10E-04	-50.37%	1090.86%
Eutrophication: Marine, fraction of nutrients reaching marine end compartment (N)	kg N - eq	5.01E-11	-4.51%	199.60%
Eutrophication: Terrestrial, accumulated exceedance (AE)	mol N - eq	2.12E-09	-22.52%	127.42%
Human toxicity: Carcinogenic, comparative toxic unit for human (CTUh)	CTUh	3.12E-03	-24.05%	19.28%
Human toxicity: Non-carcinogenic, comparative toxic unit for human (CTUh)	CTUh	1.45E-01	-57.08%	1.40%
Ionizing radiation: Human health, human exposure efficiency relative to u235	kBq - U <sup>235</sup> - eq	3.38E-06	6065.78%	979.39%
Land use, soil quality index	-	3.95E-09	24.58%	260.11%
Material resources: Metals/minerals, abiotic depletion potential (ADP): Elements (ultimate reserves)	kg Sb - eq	2.29E-09	-62.99%	-52.18%
Ozone depletion, ozone depletion potential (ODP)	kg CFC <sub>11</sub> - eq	3.99E-09	-16.37%	27.60%
Particulate matter formation, impact on human health	Diseases incident	2.26E-09	-22.04%	-15.66%
Photochemical ozone formation: Human health, tropospheric ozone concentration increase	kg NMVOX - eq	1.37E-04	-36.61%	71.55%
Water use, user deprivation potential (deprivation-weighted water consumption)	m <sup>3</sup> eq. Deprived	4.16E-05	11.55%	-21.38%

- An increase in “energy resources” consumption of +900%
- A slight decrease of climate change impacts of -9%
- A decrease of the categories “freshwater eutrophication” of -50%, “human toxicity, carcinogenic” of -57% and “material resources” of -63%

Regarding the German electricity mix from 2021, by contrast, it is principally generated by lignite coal, oil and gas, with each source

having different contributions to each impact category [83]. The employment of this mix leads to.

- An increase of “eutrophication” and “ionizing radiation” of +1000%
- An increase of “climate change” and “freshwater eutrophication” of +400% and +500%
- A decrease of material resources consumption of -50%

#### 4. Conclusions and outlook

A life cycle assessment has been carried out in order to evaluate the environmental performance of a new metal-supported PCEC developed in the ARCADE project once target values are reached. This is compared to a SOEC. According to the modeling assumptions made, the environmental performance of the metal-supported PCEC is strongly affected by the technological improvements of the PCEC which are represented by higher current density and greater faradaic efficiency. It has been demonstrated how an overall environmental impact comparable to the SOEC technology (electrolyte support) is obtained once the PCEC technological targets set by the ARCADE consortium are reached (i.e. 90% faradaic efficiency and 0.8 A/cm<sup>2</sup> current density).

The PCEC environmental profile results to be strongly impacted by the faradaic efficiency (the higher the better) while the current density degradation has little effect. When considering the complete life cycle, the environmental burden related to the stack manufacturing is negligible for all impact categories except for “human toxicity: carcinogenic”. Still, this life cycle stage has only a small contribution of 15% to this impact category. Metal-supported cells lead to a higher demand for metals, resulting in higher human toxicity impacts. These are due to carcinogenic emissions mainly linked with the metals employed in the alloy such as chromium, nickel and arsenic. A future detailed analysis of different alloy options appears advisable. Notably the acidification impact of the powder synthesis process (the Pechini process) and especially the chelating and polymerizing agents used, is very high. It could be reduced by scaling up techniques such as single step reactive sintering.

Water (steam) consumption is assumed to be the same for PCEC and SOEC (i.e. calculated according to stoichiometric reactions) due to lack of data and knowledge related to the PCEC stack steam demand and utilization. In the comparison between SOEC and PCEC technologies, especially when different steam utilizations are present, more detailed steam consumption modeling could improve the results tackling the issue linked with this uncertainty. This is advised also as next steps in future projects.

More precise information on operational performances is required in order to have more robust results for the environmental profile along the whole life cycle. A related future LCA would benefit from complementary modeling activities related to a) the scaling up of PCEC from cell to stack size b) the technical behaviour, as contact resistance or steam utilization, to provide better input data and c) the sizing of BoP components from coupling with a technical analysis, leading to final results that are more robust.

#### CRedit authorship contribution statement

**Andrea Moranti:** Writing – review & editing, Writing – original draft, Visualization, Validation, Software, Methodology, Investigation, Formal analysis, Data curation, Conceptualization. **Federico Riva:** Writing – review & editing, Visualization, Validation, Supervision, Software, Methodology, Investigation, Formal analysis, Data curation, Conceptualization. **Till M. Bachmann:** Writing – review & editing, Visualization, Validation, Supervision, Software, Resources, Project administration, Methodology, Investigation, Funding acquisition, Formal analysis, Data curation, Conceptualization. **Julian Dailly:** Writing – review & editing, Visualization, Validation, Supervision, Resources, Project administration, Methodology, Investigation, Funding

acquisition, Formal analysis, Data curation, Conceptualization.

### Declaration of competing interest

The authors declare that they have no known competing financial interests or personal relationships that could have appeared to influence the work reported in this paper.

### Abbreviations

BGLC	Barium gadolinium lanthanum cobalt
BoP	Balance of plant
BZCY	Barium cerium yttrium zirconate
GDC	Gadolinium-doped ceria
HTE	High temperature electrolysis
ISO	International organization for standardization
LCA	Life cycle assessment
LCIA	Life cycle impact assessment
LSCF	Lanthanum strontium cobalt ferrite
LSM	Lanthanum strontium manganite
LT	Long-term
MCF	Manganese cobalt ferrite
NiO	Nickel
PCC	Protonic ceramic cell
PCEC	Protonic ceramic electrolyzer cell
RES	Renewable energy sources
SMR	Steam methane reforming
SOC	Solid oxide cell
SOEC	Solid oxide electrolyzer cell
SRU	Single repeating unit
TRL	Technological readiness level

### Appendix A. Supplementary data

Supplementary data to this article can be found online at <https://doi.org/10.1016/j.ijhydene.2024.10.221>.

### References

- Ang T-Z, Salem M, Kamarol M, Das HS, Nazari MA, Prabaharan N. A comprehensive study of renewable energy sources: classifications, challenges and suggestions. *Energy Strategy Rev* 2022;43:100939. <https://doi.org/10.1016/j.esr.2022.100939>.
- Utgikar V, Thiesen T. Life cycle assessment of high temperature electrolysis for hydrogen production via nuclear energy. *Int J Hydrogen Energy* 2006;31:939–44. <https://doi.org/10.1016/j.ijhydene.2005.07.001>.
- Hauch A, Küngas R, Blennow P, Hansen AB, Hansen JB, Mathiesen BV, et al. Recent advances in solid oxide cell technology for electrolysis. *Science* 2020;370:eaba6118. <https://doi.org/10.1126/science.aba6118>. 1979.
- Duan C, Kee R, Zhu H, Sullivan N, Zhu L, Bian L, et al. Highly efficient reversible protonic ceramic electrochemical cells for power generation and fuel production. *Nat Energy* 2019;4:230–40. <https://doi.org/10.1038/s41560-019-0333-2>.
- Choi S, Davenport TC, Haile SM. Protonic ceramic electrochemical cells for hydrogen production and electricity generation: exceptional reversibility, stability, and demonstrated faradaic efficiency. *Energy Environ Sci* 2019;12:206–15. <https://doi.org/10.1039/C8EE02865F>.
- Le LQ, Meisel C, Hernandez CH, Huang J, Kim Y, O'Hayre R, et al. Performance degradation in proton-conducting ceramic fuel cell and electrolyzer stacks. *J Power Sources* 2022;537:231356. <https://doi.org/10.1016/j.jpowsour.2022.231356>.
- Ferrero D, Lanzini A, Santarelli M, Leone P. A comparative assessment on hydrogen production from low- and high-temperature electrolysis. *Int J Hydrogen Energy* 2013;38:3523–36. <https://doi.org/10.1016/j.ijhydene.2013.01.065>.
- Hauch A, Küngas R, Blennow P, Hansen AB, Hansen JB, Mathiesen BV, et al. [improvement cell performance 2,5] Recent advances in solid oxide cell technology for electrolysis. *Science* 2020;370. <https://doi.org/10.1126/science.aba6118>. eaba6118–eaba6118, (1979).
- Bello IT, Zhai S, He Q, Cheng C, Dai Y, Chen B, et al. Materials development and prospective for protonic ceramic fuel cells. *Int J Energy Res* 2022;46:2212–40. <https://doi.org/10.1002/er.7371>.
- Dubois A, Ricote S, Braun RJ. [PCC Manufacturing+stack price] Benchmarking the expected stack manufacturing cost of next generation, intermediate-temperature protonic ceramic fuel cells with solid oxide fuel cell technology. *J Power Sources* 2017;369:65–77. <https://doi.org/10.1016/j.jpowsour.2017.09.024>.
- Le LQ, Hernandez CH, Rodriguez MH, Zhu L, Duan C, Ding H, et al. Proton-conducting ceramic fuel cells: scale up and stack integration. *J Power Sources* 2021;482:228868. <https://doi.org/10.1016/j.jpowsour.2020.228868>.
- Lee S-S, Hong T-W. Life cycle assessment for proton conducting ceramics synthesized by the sol-gel process. *Materials* 2014;7:6677–85. <https://doi.org/10.3390/ma7096677>.
- SUNFIRE-HYLINK SOEC datasheet. 2023.
- Kee RJ, Ricote S, Zhu H, Braun RJ, Carins G, Persky JE. [SOEC\_inlet T steam] perspectives on technical challenges and scaling considerations for tubular protonic-ceramic electrolysis cells and stacks. *J Electrochem Soc* 2022;169:54525. <https://doi.org/10.1149/1945-7111/ac6c4e>.
- Hagen A, Caldugno R, Capotondo F, Sun X. Metal supported electrolysis cells. *Energies* 2022;15. <https://doi.org/10.3390/en15062045>.
- Stange M, Stefan E, Denonville C, Larring Y, Rørvik PM, Haugrud R. Development of novel metal-supported proton ceramic electrolyser cell with thin film BZY15–Ni electrode and BZY15 electrolyte. *Int J Hydrogen Energy* 2017;42:13454–62. <https://doi.org/10.1016/j.ijhydene.2017.03.028>.
- Sata N, Costa R. Protonic ceramic electrochemical cells in a metal supported architecture: challenges, status and prospects. *Progress in Energy* 2024;6:32002. <https://doi.org/10.1088/2516-1083/ad3f6b>.
- Bernadet L, Moncasi C, Torrell M, Tarancón A. High-performing electrolyte-supported symmetrical solid oxide electrolysis cells operating under steam electrolysis and co-electrolysis modes. *Int J Hydrogen Energy* 2020;45:14208–17. <https://doi.org/10.1016/j.ijhydene.2020.03.144>.
- Schiller G, Ansar A, Lang M, Patz O. High temperature water electrolysis using metal supported solid oxide electrolyser cells (SOEC). *J Appl Electrochem* 2009;39:293–301. <https://doi.org/10.1007/s10800-008-9672-6>.
- Hellweg S, Milà i Canals L. Emerging approaches, challenges and opportunities in life cycle assessment. *Science* 2014;344:1109–13. <https://doi.org/10.1126/science.1248361>. 1979.
- Eisenberg DA, Yu M, Lam CW, Oguneitan OA, Schoenung JM. Comparative alternative materials assessment to screen toxicity hazards in the life cycle of CIGS thin film photovoltaics. *J Hazard Mater* 2013;260:534–42. <https://doi.org/10.1016/j.jhazmat.2013.06.007>.
- Patyk A, Bachmann TM, Brisse A. Life cycle assessment of H<sub>2</sub> generation with high temperature electrolysis. *Int J Hydrogen Energy* 2013;38:3865–80. <https://doi.org/10.1016/j.ijhydene.2013.01.063>.

- [23] Karakoussis V, Brandon NP, Leach M, van der Vorst R. The environmental impact of manufacturing planar and tubular solid oxide fuel cells. *J Power Sources* 2001; 101:10–26. [https://doi.org/10.1016/S0378-7753\(01\)00482-7](https://doi.org/10.1016/S0378-7753(01)00482-7).
- [24] Giraldi MR, François J-L, Martin-del-Campo C. Life cycle assessment of hydrogen production from a high temperature electrolysis process coupled to a high temperature gas nuclear reactor. *Int J Hydrogen Energy* 2015;40:4019–33. <https://doi.org/10.1016/j.ijhydene.2015.01.093>.
- [25] Häfele S, Hauck M, Dailly J. Life cycle assessment of the manufacture and operation of solid oxide electrolyser components and stacks. *Int J Hydrogen Energy* 2016;41:13786–96. <https://doi.org/10.1016/j.ijhydene.2016.05.069>.
- [26] Lozanovski A, Schuller O, Faltenbacher Reviewer M, Board A, Fullana Palmer PI, Bode M, et al. Guidance document for performing LCAs on fuel cells and H<sub>2</sub> technologies guidance document for performing LCA on hydrogen production systems deliverable d3.3-final guidance document work package 3-preparation and consultation of the guidance document approved by the X external reviewer X work package leader X project coordinator o European commission/FCH ju. [n.d].
- [27] Ökobilanz-software (LCA) | Umberto [n.d].
- [28] Choi S, Davenport TC, Haile SM. [PBSCF-BZCYYb(also ely)] Protonic ceramic electrochemical cells for hydrogen production and electricity generation: exceptional reversibility, stability, and demonstrated faradaic efficiency. *Energy Environ Sci* 2019;12:206–15. <https://doi.org/10.1039/C8EE02865F>.
- [29] Chen K, Dong D, Jiang SP. Hydrogen production from water and air through solid oxide electrolysis. In: Fang Z, Smith Richard L Jr, Qi X, editors. *Production of hydrogen from renewable resources*. Dordrecht: Springer Netherlands; 2015. p. 223–48. [https://doi.org/10.1007/978-94-017-7330-0\\_8](https://doi.org/10.1007/978-94-017-7330-0_8).
- [30] *Hydrogenics. Annex pem 1MW hydrogen plant - HiLYZER 200/30. 2019.*
- [31] Bareiß K, de la Rua C, Möckl M, Hamacher T. Life cycle assessment of hydrogen from proton exchange membrane water electrolysis in future energy systems. *Appl Energy* 2019;237:862–72. <https://doi.org/10.1016/j.apenergy.2019.01.001>.
- [32] Cohen S, Porter S, Chow O, Henderson D. *Hydrogen generation from electrolysis*. Proton Energy Systems 2009.
- [33] Sulzer Chemtech. *Gas-Liquid Separation Technology*, p. 25 n.d. <https://www.sulzer.com/en/products/separation-technology/separators> (accessed September 9, 2023).
- [34] Karakoussis V, Brandon NP, Leach M, van der Vorst R. The environmental impact of manufacturing planar and tubular solid oxide fuel cells. *J Power Sources* 2001; 101:10–26. [https://doi.org/10.1016/S0378-7753\(01\)00482-7](https://doi.org/10.1016/S0378-7753(01)00482-7).
- [35] *Catalysts B. Basf - catalyst Pd/AS. 2024.*
- [36] Praxaidos. Deoxo System n.d. <http://www.praxaidos.com/deoxo-system/> (accessed September 9, 2023).
- [37] Althaus H-J, Hischer R, Doka G, Dones R, Heck T, Hellweg S, et al. *Overview and methodology Data v20 (2007) Ecoinvent report No 1. Switzerland. 2007.*
- [38] JRC-IES. *International reference life cycle data system (ILCD) handbook: general guide for life cycle assessment - detailed guidance. 2010.*
- [39] *ISO. Environmental management—life cycle assessment—requirement and guidelines. ISO; 2006, 14044. S(2006b).*
- [40] Lithako A, Oboirien B, Patel B. Life cycle assessment of Power-to-Gas (PtG) technology – evaluation of system configurations of renewable hydrogen and methane production. *Sustain Energy Technol Assessments* 2023;60:103527. <https://doi.org/10.1016/j.seta.2023.103527>.
- [41] Commission European, Research Centre Joint, Pilenga A, Tsoitridis G. *EU harmonised terminology for low temperature water electrolysis for energy storage applications*. Publications Office; 2018. <https://doi.org/10.2760/138987>.
- [42] Osman AI, Mehta N, Elgarahy AM, Hefny M, Al-Hinai A, Al-Muhtaseb AH, et al. Hydrogen production, storage, utilisation and environmental impacts: a review. *Environ Chem Lett* 2022;20:153–88. <https://doi.org/10.1007/s10311-021-01322-8>.
- [43] Schmidt O, Gambhir A, Staffell I, Hawkes A, Nelson J, Few S. Future cost and performance of water electrolysis: an expert elicitation study. *Int J Hydrogen Energy* 2017;42:30470–92. <https://doi.org/10.1016/j.ijhydene.2017.10.045>.
- [44] Dimesso L. *Pechini Processes: An Alternate Approach of the Sol–Gel Method, Preparation, Properties, and Applications* 2016:1. [https://doi.org/10.1007/978-3-319-19454-7\\_123-1\\_22](https://doi.org/10.1007/978-3-319-19454-7_123-1_22).
- [45] Laue W, Thiemann M, Scheibler E, Wiegand KW. *Nitrates and nitrites*. Ullmann's encyclopedia of industrial chemistry. Wiley; 2000. [https://doi.org/10.1002/14356007.a17\\_265](https://doi.org/10.1002/14356007.a17_265).
- [46] Gaidajis G, Kakani I. Life cycle assessment of nitrate and compound fertilizers production—a case study. *Sustainability* 2021;13. <https://doi.org/10.3390/su13010148>.
- [47] Arbor A. *Building an LCA inventory: a worked example on a CO<sub>2</sub> to fertilizer process. 2020.*
- [48] Rosli AZ, Somalu MR, Osman N, Hamid NA. [Sol Gel LSCF 1] Physical characterization of LSCF-NiO as cathode material for intermediate temperature solid oxide fuel cell (IT-SOFCs). *Mater Today Proc* 2021;46:1895–900. <https://doi.org/10.1016/j.matpr.2021.01.778>.
- [49] Hajizadeh-Oghaz M, Razavi RS, Estarki ML. [Pechini] Large-scale synthesis of YSZ nanopowder by Pechini method. *Bull Mater Sci* 2014;37:969–73. <https://doi.org/10.1007/s12034-014-0033-2>.
- [50] Wang M, Su C, Zhu Z, Wang H, Ge L. [BSCF-BZCYYb3] Composite cathodes for protonic ceramic fuel cells: rationales and materials. *Compos B Eng* 2022;238: 109881. <https://doi.org/10.1016/j.compositesb.2022.109881>.
- [51] Barison S, Battagliarin M, Cavallin T, Doubova L, Fabrizio M, Mortalò C, et al. High conductivity and chemical stability of BaCe<sub>1-x-y</sub>Zr<sub>x</sub>Y<sub>0.3</sub>O<sub>3-δ</sub> proton conductors prepared by a sol–gel method. *J Mater Chem* 2008;18:5120–8. <https://doi.org/10.1039/B808344D>.
- [52] Niwa E, Kluczny M, Kim HY, Song JT, Watanabe M, Takagaki A, et al. Proton conductivity in Yb-doped BaZrO<sub>3</sub>-based thin film prepared by pulsed laser deposition. *Solid State Ionics* 2023;396:116240. <https://doi.org/10.1016/j.ssi.2023.116240>.
- [53] Chen X, Zhang H, Li Y, Xing J, Zhang Z, Ding X, et al. [LSCF-BZCYYb3] Fabrication and performance of anode-supported proton conducting solid oxide fuel cells based on BaZr<sub>0.1</sub>Ce<sub>0.7</sub>Y<sub>0.1</sub>Yb<sub>0.1</sub>O<sub>3-δ</sub> electrolyte by multi-layer aqueous-based co-tape casting. *J Power Sources* 2021;506:229922. <https://doi.org/10.1016/j.jpowsour.2021.229922>.
- [54] Mason TO. *Traditional ceramics | clay, glazing & firing techniques. 1998.*
- [55] Zyguntowicz J, Gizowska M, Tomaszewska J, Piotrkiewicz P, Zurowski R, Wachowski M, et al. [1,5% losses of slip casting] sintering behavior, thermal expansion, and environmental impacts accompanying materials of the Al<sub>2</sub>O<sub>3</sub>/ZrO<sub>2</sub> system fabricated via slip casting. *Materials* 2021;14. <https://doi.org/10.3390/ma14123365>.
- [56] Zhang Y, Zeng F, Yu C, Wu C, Ding W, Lu X. Fabrication and characterization of dense BaCo<sub>0.7</sub>Fe<sub>0.2</sub>Nb<sub>0.1</sub>O<sub>3-δ</sub> tubular membrane by slip casting techniques. *Ceram Int* 2015;41:1401–11. <https://doi.org/10.1016/j.ceramint.2014.09.073>.
- [57] Xiao Y, Wang M, Bao D, Wang Z, Jin F, Wang Y, et al. [Slip casting slurry anode] performance of fuel electrode-supported tubular protonic ceramic cells prepared through slip casting and dip-coating methods. *Catalysts* 2023;13. <https://doi.org/10.3390/catal13010182>.
- [58] Somalu MR, Muchtar A, Daud WRW, Brandon NP. [Solvent/Binder screen printing] Screen-printing inks for the fabrication of solid oxide fuel cell films: a review. *Renew Sustain Energy Rev* 2017;75:426–39. <https://doi.org/10.1016/j.rser.2016.11.008>.
- [59] Suresh RR, Lakshmanakumar M, Arockia Jayalatha JBB, Rajan KS, Sethuraman S, Krishnan UM, et al. Fabrication of screen-printed electrodes: opportunities and challenges. *J Mater Sci* 2021;56:8951–9006. <https://doi.org/10.1007/s10853-020-05499-1>.
- [60] Somalu MR, Muchtar A, Daud WRW, Brandon NP. [Screen printing solvent ratio+solid content] Screen-printing inks for the fabrication of solid oxide fuel cell films: a review. *Renew Sustain Energy Rev* 2017;75:426–39. <https://doi.org/10.1016/j.rser.2016.11.008>.
- [61] Somalu MR, Yufit V, Brandon NP. [Screen printing minimum solid and ethyl cellulose binder] The effect of solids loading on the screen-printing and properties of nickel/scandia-stabilized-zirconia anodes for solid oxide fuel cells. *Int J Hydrogen Energy* 2013;38:9500–10. <https://doi.org/10.1016/j.ijhydene.2012.06.061>.
- [62] *Kdmfab. Understanding the pvd coating process: a step-by-step guide. 2023.*
- [63] Baptista A, Silva F, Porteiro J, Miguez J, Pinto G. Sputtering physical vapour deposition (pvd) coatings: a critical review on process improvement and market trend demands. *Coatings* 2018;8. <https://doi.org/10.3390/coatings8110402>.
- [64] Coddet P, Liao H, Coddet C. A review on high power SOFC electrolyte layer manufacturing using thermal spray and physical vapour deposition technologies. *Adv Manuf* 2014;2:212–21. <https://doi.org/10.1007/s40436-013-0049-7>.
- [65] Fan L, Xie H, Su P-C. Spray coating of dense proton-conducting BaCe<sub>0.7</sub>Zr<sub>0.1</sub>Y<sub>0.2</sub>O<sub>3</sub> electrolyte for low temperature solid oxide fuel cells. *Int J Hydrogen Energy* 2016;41:6516–25. <https://doi.org/10.1016/j.ijhydene.2016.03.001>.
- [66] Parra D, Patel MK. Techno-economic implications of the electrolyser technology and size for power-to-gas systems. *Int J Hydrogen Energy* 2016;41:3748–61. <https://doi.org/10.1016/j.ijhydene.2015.12.160>.
- [67] Zhao G, Kraglund MR, Frandsen HL, Wulff AC, Jensen SH, Chen M, et al. Life cycle assessment of H<sub>2</sub>O electrolysis technologies. *Int J Hydrogen Energy* 2020;45: 23765–81. <https://doi.org/10.1016/j.ijhydene.2020.05.282>.
- [68] Kee RJ, Ricote S, Zhu H, Braun RJ, Carins G, Persky JE. [BOP SOEC] Perspectives on technical challenges and scaling considerations for tubular protonic-ceramic electrolysis cells and stacks. *J Electrochem Soc* 2022;169:54525. <https://doi.org/10.1149/1945-7111/ac6c4e>.
- [69] Bui T, Lee D, Ahn KY, Kim YS. Techno-economic analysis of high-power solid oxide electrolysis cell system. *Energy Convers Manag* 2023;278:116704. <https://doi.org/10.1016/j.enconman.2023.116704>.
- [70] Staffell I, Ingram A, Kendall K. Energy and carbon payback times for solid oxide fuel cell based domestic CHP. *Int J Hydrogen Energy* 2012;37:2509–23. <https://doi.org/10.1016/j.ijhydene.2011.10.060>.
- [71] *Satcon. Inverter fotovoltaici | PowerGate plus 500 kW. 2010.*
- [72] ABB central inverters PVS980-58-4348 to 5000 kVA. [n.d].
- [73] *SUNFIRE-HYLINK SOEC. [n.d].*
- [74] Patyk A, Bachmann TM, Brisse A. Life cycle assessment of H<sub>2</sub> generation with high temperature electrolysis. *Int J Hydrogen Energy* 2013;38:3865–80. <https://doi.org/10.1016/j.ijhydene.2013.01.063>.
- [75] *Filtration Ltd W. Water separators. [n.d].*
- [76] Kural S, Ayvaz M. The ballistic behavior of type 1 metallic pressurized hydrogen storage tanks against ballistic threats. *Int J Hydrogen Energy* 2018;43:20284–92. <https://doi.org/10.1016/j.ijhydene.2018.06.126>.
- [77] EATON. *Gas Liquid Separators* n.d. <https://www.eaton.com/gb/en-gb/products/filteration-solutions/filter-systems/gas-liquid-separator.html> (accessed September 1, 2024).
- [78] Boegger. *Demister pads – ideal for gas and liquid separating and filtering* n.d. <https://www.structuredpacking.org/structured-packing/demister-pads.html> (accessed September 9, 2023).
- [79] Kim T, Song Y, Kang J, Kim SK, Kim S. A review of recent advances in hydrogen purification for selective removal of oxygen: deoxo catalysts and reactor systems. *Int J Hydrogen Energy* 2022;47:24817–34. <https://doi.org/10.1016/j.ijhydene.2022.05.221>.

- [80] EcoVapor. Oxygen Removal from Biogas (deoxo) n.d. <https://ecovaporrs.com/biogas-purification-solutions/zero2-oxygen-removal-biogas/>. [Accessed 4 September 2023].
- [81] Fraunhofer ISE. Study: current and future cost of photovoltaics. 2015.
- [82] Sangwongwanich A, Yang Y, Sera D, Blaabjerg F, Zhou D. On the impacts of PV array sizing on the inverter reliability and lifetime. *IEEE Trans Ind Appl* 2018;54: 3656–67. <https://doi.org/10.1109/TIA.2018.2825955>.
- [83] Haque N. 29 - the life cycle assessment of various energy technologies. In: Letcher TM, editor. *Future energy*. third ed.). third ed. Elsevier; 2020. p. 633–47. <https://doi.org/10.1016/B978-0-08-102886-5.00029-3>.